Journal of Luminescence 224 (2020) 117309

Contents lists available at ScienceDirect

Journal of Luminescence

journal homepage: http://www.elsevier.com/locate/jlumin

Thiophene-derivatized pyridine-biscarboxamide as a sensitizer for Ln^{III} luminescence and $^1O_2$ generation

Katherine R. Johnson, Manuel A. Gracia-Nava, Ana de Bettencourt-Dias *

Department of Chemistry, University of Nevada, Reno, 1664 N. Virginia Street, Reno, NV, 89557, USA

ARTICLE INFO

Keywords:
Lanthanide luminescence
Coordination complexes
Singlet oxygen generation
Dual-functionality

ABSTRACT

Lanthanide ion (Ln^{III} = Gd^{III}, Eu^{III}, Nd^{III}, Er^{III}, and Yb^{III}) complexes of 4-thiophen-3-yl-pyridine-2,6-dicarboxamide (1Tcbx) were isolated and their photophysical properties explored. In acetonitrile, 1Tcbx sensitizes the visible and NIR-emitting Ln^{III} (Ln^{III} = Eu^{III}, Yb^{III}, Nd^{III}, and Er^{III}) ions. Quantum yields of Ln^{III} sensitization are φ^{Eu} = 25%, φ^{Yb} = 0.42%, φ^{Nd} = 0.19%, and φ^{Er} = 0.01%. These luminescent complexes generate singlet oxygen ($^1O_2$) as well, which is monitored through its phosphorescence at 1270 nm. For the Nd^{III} complex, the formation of $^1O_2$ was masked by the intense $^4F_{3/2} \rightarrow {}^4I_{13/2}$ transition. The efficiency of $^1O_2$ generation (φ_{1O2}) was quantified for $[Gd(1Tcbx)_3]^{3+}$ at 12%.

1. Introduction

Luminescent lanthanide (Ln^{III}) complexes are interesting for applications in sensing and imaging [1–15]. The spectroscopic properties of Ln^{III}, namely long excited-state lifetimes and sharp emission bands, arise from 4*f*-4*f* transitions and enable the use of time-gated detection for improved signal-to-noise ratio. Due to the low molar absorptivity of these electronic transitions ($\varepsilon < 10\ M^{-1}\ cm^{-1}$), direct excitation of the Ln^{III} is inefficient. Therefore, organic chromophores are used as sensitizer in a process called the *antenna effect*. This process, shown in Fig. 1, begins with the population of the ligand excited singlet state, ^1S, upon light irradiation ($h\nu$). Subsequent intersystem crossing (ISC) populates a triplet state, ^3T, a long-lived state that can energy transfer (ET) to the emissive excited state of the Ln^{III} ion (**f*). Ln^{III}-centered luminescence returns the metal ion to the ground state (*f*) [16]. While it is generally accepted that the main pathway of sensitization is through the ^3T state, concurrent or alternative sensitization through ^1S is reported as well [17,18]. In addition, sensitization through charge transfer states (CT) has gained increasing attention [19].

Targeted functionalization of the antennas can be useful to tune Ln^{III} complexes for specific properties, and thus, allows for blending additional functionality with the unique characteristics of Ln^{III} luminescence. For example, a Tb^{III} complex derivatized with a borate group is a poor sensitizer of Tb^{III} luminescence, yet upon reaction with H_2O_2 generates a phenol capable of transferring energy in a turn-on luminescence process useful to sense the peroxide species *in situ* [20]. A hetero-Ln^{III} coordination polymer with bridging 5-benzene-1,4-dicarboxylato groups exhibits white light luminescence with increased thermal stability [21].

More recently, Ln^{III} luminescent molecules have been described that generate cytotoxic singlet oxygen ($^1O_2$). As shown in Fig. 1, $^1O_2$ can be formed upon energy transfer between the ^3T state and triplet oxygen ($^3O_2$). Due to the role of the ^3T state in the sensitization of Ln^{III}-centered emission and $^1O_2$ generation, these two pathways are concurrent and will influence each other. Some examples of $^1O_2$ generating luminescent Ln^{III} complexes feature ligands functionalized with pyrene [22], porphyrin [23], polycyclic aromatic compounds [24], quinoline [25], 1,4,7-triazacyclonane [26], nitrogen-containing herterocycles [27], and hypocrellin B [28]. Our group has described a naphthalimide-based photosensitizer; its resulting complexes are capable of either visible (Eu^{III}) or near-infrared (NIR) luminescence (Yb^{III} or Nd^{III}), in addition to generating $^1O_2$ [29]. We have also recently described a 2,2′:5′,2″-terthiophene-based antenna for Ln^{III} emission and $^1O_2$ generation, 3Tcbx. We demonstrated that this ligand is capable of sensitizing the NIR luminescence of Yb^{III}, Nd^{III}, and Er^{III} and of wavelength-dependent $^1O_2$ generation, due to the involvement of higher energy excited states on the ligand [30]. Further, our group has described oligothiophene-based water-soluble complexes that sensitize visible (Eu^{III}) and NIR luminescence (Yb^{III}, Nd^{III}) and are phototoxic to HeLa cells [31]. Although these examples do demonstrate Ln^{III} luminescence and $^1O_2$ generation capability, in many cases the efficiencies of these processes are low, and sensitization of Ln^{III} luminescence is weak in the presence of $^3O_2$ [24].

* Corresponding author.
E-mail address: abd@unr.edu (A. de Bettencourt-Dias).

https://doi.org/10.1016/j.jlumin.2020.117309
Received 5 March 2020; Received in revised form 16 April 2020; Accepted 20 April 2020
Available online 25 April 2020

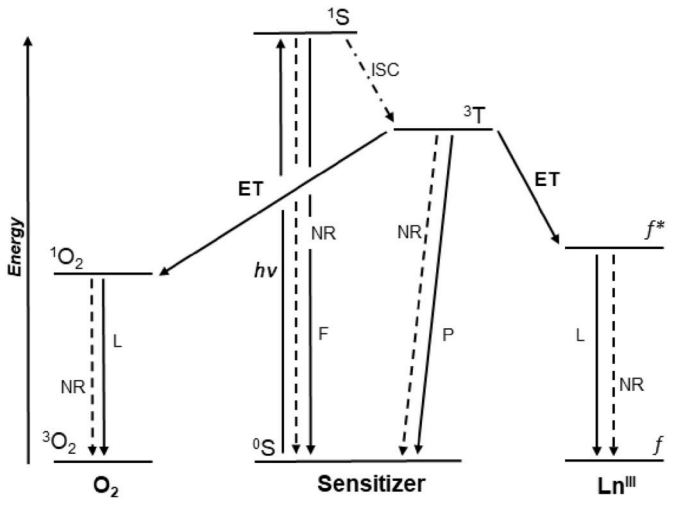

Fig. 1. Energy level diagram illustrating the energy transfer (ET) processes for Ln^{III} ion sensitization and $^1O_2$ generation. Energy hυ is absorbed by the ligand and populates a singlet excited state (^{1}S). A triplet excited state (^{3}T) is populated after intersystem crossing (ISC). ^{3}T can transfer energy to the emissive f* excited state, which decays by luminescence (L) to the ground state. In the presence of $^3O_2$, the ^{3}T can lead to $^1O_2$ generation as well. Nonradiative (NR) (dash-dot lines) pathways can lead to quenching of excited states. Other possible radiative processes are fluorescence (F) and phosphorescence (P). Energy levels are not drawn to scale.

To better control our ability to generate $^1O_2$ efficiently, without sacrificing the benefit of Ln^{III} luminescence, it is advantageous to expand our knowledge of other $^1O_2$ generating functional groups.

Oligohiophene-based compounds, such as 2,2':5',2''-terthiophene, have been studied for their antibiotic [32], insecticidal [33–36], antifungal [37,38], and antiviral [39–41] properties, which occur as a result of the compounds' ability to generate $^1O_2$. Thiophene and methylthiophene can generate $^1O_2$ as well, as verified by *ab initio* calculations [42]. Our group has isolated thiophene-based Ln^{III} chelators [30,43–45], some of which show promising Ln^{III} luminescence properties, with efficiencies for Eu^{III} and Tb^{III} emission of 76% and 59%, respectively [46]. We have thus isolated a similar Ln^{III} chelator functionalized with thiophene, 1Tcbx, and its Ln^{III} (Ln^{III} = Eu^{III}, Gd^{III}, Nd^{III}, Yb^{III}, or Er^{III}) complexes, to assess their ability to concurrently luminesce and generate $^1O_2$. We observed $^1O_2$ generation and sensitized Ln^{III} luminescence in the visible with $[Eu(1Tcbx)_3]^{3+}$ and the NIR with $[Yb(1Tcbx)_3]^{3+}$, $[Nd(1Tcbx)_3]^{3+}$, and $[Er(1Tcbx)_3]^{3+}$.

2. Experimental section

2.1. Materials and methods

All commercially obtained reagents were of analytical grade and were used as received. Solvents were dried and purified by standard methods unless otherwise noted. All synthetic steps were completed under N_2 unless otherwise specified.

Nuclear Magnetic Resonance (NMR) spectroscopy. NMR spectra were recorded on Varian 400 and 500 MHz spectrometers at 25.0 ± 0.1 °C with chemical shifts reported (δ, ppm) against tetramethylsilane (TMS, 0.00 ppm).

Mass spectrometry. Electrospray ionization mass spectra (ESI-MS) were collected in positive ion mode on a Waters Micromass ZQ quadrupole in the low-resolution mode for 1Tcbx and on an Agilent model G6230A with a QTOF analyzer in the high-resolution mode for the respective metal complexes. The samples were prepared by diluting the compounds in acetonitrile solutions to a concentration of ~0.5 mg/mL and passing through a 0.2 mm microfilter.

Absorption spectroscopy. Absorption spectra were measured on a Perkin Elmer Lambda 35 spectrometer equipped with deuterium and tungsten halogen lamps (Perkin Elmer) and a concave grating with 1053 lines/mm. They were collected using a scan speed of 480 nm/min in the range of 225–600 nm with a photodiode detector. All spectra were background corrected, using solvent as the blank. Spectra of 1Tcbx and its complexes were collected at 25.0 ± 0.1 °C.

Excitation and emission spectroscopy and lifetime measurements. Emission and excitation spectra of 1Tcbx and its Ln^{III} complexes were obtained at 25.0 ± 0.1 °C in a Fluorolog-3 fluorimeter (Horiba FL3-22-iHR550), with a 1200 grooves/mm excitation monochromator with gratings blazed at 330 nm and 1200 grooves/mm or a 600 grooves/mm emission monochromator with gratings blazed at 500 nm or 1000 nm for the UV–Vis or NIR range, respectively. An ozone-free xenon lamp of 450 W (Ushio) was used as the radiation source. The excitation spectra were measured between 250 and 600 nm. The emission spectra were measured in the range of 350–800 nm using a Hamamatsu 928 P detector and in the range of 800–1600 nm using a Hamamatsu 5509-73 detector cooled with liquid N_2. All excitation and emission spectra were corrected for instrumental function. The emission decay curves were obtained using a TCSPC system and a Xe pulsed lamp as excitation source.

2.2. Synthesis of 1Tcbx

4-Bromo-N,N,N',N'-tetraethyl-2,6-pyridinedicarboxamide (1). This compound was synthesized following a modified literature procedure [47]. PBr_3 (3.3 mL, 35 mmol) was added dropwise to a solution of Br_2 (1.8 mL, 35 mmol) in petroleum ether (50 mL) at 0 °C. The solvent was decanted after complete precipitation of PBr_5, which was used without further purification. Chelidamic acid monohydrate (2.0 g, 10 mmol) was added to the PBr_5, and the melt was heated to 85 °C for 12 h. Once cooled to room temperature (RT), dry dichloromethane (DCM, 40 mL) was added and stirred until dissolved. Next, the reaction was cooled to 0 °C, and diethylamine (5.0 mL, 48 mmol) was added dropwise. After stirring at 0 °C for 1 h, the reaction mixture was warmed to 45 °C for 1.5 h. The reaction was cooled to RT, and quenched with saturated $NaHCO_3$ (50 mL). The desired product was extracted with DCM (3 × 15 mL), washed with water (3 × 50 mL), and dried over anhydrous Na_2SO_4. After filtration, the remaining solvent was removed under reduced pressure and the final product was recrystallized as a white solid from *n*-hexanes. Yield: 2.8 g (79%). ^{1}H NMR ($CDCl_3$, 400 MHz) δ (ppm): 1.15 (*t*, *J* = 7.1 Hz, 6H), 1.24 (*t*, *J* = 7.1 Hz, 6H), 3.33 (*q*, *J* = 7.0 Hz, 4H), 3.55 (*q*, *J* = 7.0 Hz, 4H), 7.79 (*s*, 1H).

2-Thiopheneboronic acid (2). This compound was synthesized following a modified literature procedure [48]. 2-Bromothiophene (1.0 mL, 3.6 mmol) was dissolved in tetrahydrofuran (THF, 20 mL) and cooled to −78 °C. *N*-butyllithium (4.0 mL, 4.8 mmol,1.2 M in hexane) and triisopropyl borate (1.1 mL, 4.8 mmol) were added sequentially to the reaction. After stirring for 4 h, the reaction was quenched with 1 M HCl (20 mL) and extracted with DCM (3 × 15 mL). The combined organic layers were washed with water (3 × 10 mL) and brine (3 × 10 mL). DCM was removed under reduced pressure and the final product was recrystallized from 1:1 hexane:benzene. Yield: 330 mg (71%) – white solid. ^{1}H NMR (DMSO-d_6, 400 MHz) δ (ppm): 7.16 (*m*, *J* = 4.7, 3.4 Hz, 1H), 7.67 (*d*, *J* = 4.7 Hz, 1H), 7.73 (*d*, *J* = 4.7 Hz, 1H), 8.16 (*s*, 2H).

4-(2-Thienyl)-N,N,N',N'-tetraethyl-2,6-pyridinedicarboxamide (1Tcbx). Compounds *1* (170 mg, 0.48 mmol), *2* (60 mg, 0.48 mmol), K_2CO_3 (230 mg, 1.15 mmol), and $[Pd(PPh_3)_4]$ (40 mg, 0.04 mmol) were dissolved in *N,N*-dimethylformamide (DMF) (10 mL) and heated at 80 °C for 22 h. The mixture was quenched with water and extracted with $CHCl_3$ (3 × 35 mL). The organic layers were combined, washed with water (3 × 50 mL) and brine (3 × 50 mL), dried over anhydrous $MgSO_4$, and filtered. The solvent was removed under reduced pressure and the resulting product was purified on a flash silica column using ethyl acetate as the eluent. Yield: 140 mg (81%) – white solid. ^{1}H NMR (400 MHz, $CDCl_3$) δ (ppm): 1.16 (*t*, *J* = 7.1 Hz, 6H), 1.27 (*t*, *J* = 7.1 Hz, 6H), 3.37 (*q*,

$J = 7.1$ Hz, 4H), 3.57 (*q*, $J = 7.1$ Hz, 4H), 7.13 (*m*, $J = 5.1$, 3.7 Hz, 1H), 7.45 (*dd*, $J = 3.7$, 1.1 Hz, 1H), 7.57 (*dd*, $J = 3.7$, 1.1 Hz, 1H), 7.79 (*s*, 2H).^{13}C NMR (100 MHz, $CDCl_3$) δ (ppm): 12.80, 14.28, 40.20, 43.29, 119.66, 126.22, 128.03, 128.57, 140.24, 143.60, 154.33, 168.00. ESI-MS: $[M+H]^+$ *m/z*: 360 (exp.) 360 (calc.).

2.3. Speciation studies

The speciation of the complexes of 1Tcbx was determined through UV–Vis absorption spectroscopy in spectrophotometric grade acetonitrile at 25.0 ± 0.1 °C. Solutions of 1Tcbx and $Ln(NO_3)_3$ (Ln = Eu^{III}, Nd^{III}, or Yb^{III}) with a wide range of stoichiometric ratios were prepared, and their absorption spectra measured. The stability constants were refined using HypSpec2014 [49]. The speciation diagrams were generated using HySS [50].

2.4. Synthesis of $[Ln(1Tcbx)_3]^{3+}$

All metal complexes were prepared by mixing one equivalent of dry $Ln(NO_3)_3$ (Ln^{III} = Eu^{III}, Yb^{III}, Nd^{III}, Gd^{III} or Er^{III}) with 3 equivalents of 1Tcbx in acetonitrile and refluxing for 16 h. The solvent was removed under reduced pressure. The resulting white solids were dried under reduced pressure.

$[Eu(1Tcbx)_3(NO_3)_2]^+$ ESI-MS: *m/z*: 1354.4045 (calc) 1354.4461 (exp); Yield: 95%

$[Yb(1Tcbx)_3(NO_3)_2]^+$ ESI-MS: *m/z*: 1375.4142 (calc) 1375.4798 (exp); Yield: 94%

$[Nd(1Tcbx)_3(NO_3)_2]^+$ ESI-MS: *m/z*: 1343.3830 (calc) 1343.4001 (exp); Yield: 97%

$[Er(1Tcbx)_3(NO_3)_2]^+$ ESI-MS: *m/z*: 1369.4046 (calc) 1369.4210 (exp); Yield: 92%

$[Gd(1Tcbx)_3(NO_3)_2]^+$ ESI-MS: *m/z*: 1359.3996 (calc) 1359.4634 (exp). Yield: 92%

2.5. X-ray crystallography

Crystal data, data collection, and refinement details for 1Tcbx are given below. A suitable crystal was mounted on a glass fiber and placed in the low-temperature nitrogen stream of a Bruker SMART CCD area detector diffractometer. A full sphere of data was collected using a graphite-monochromated Mo-Kα radiation source (λ = 0.71073 Å). Multi-scan absorption corrections were applied using SADABS [51]. The structure was solved by direct methods and refined by least-square methods on F [2] using the SHELXTL [52] programming package. All non-hydrogen atoms were refined anisotropically, and the hydrogen atoms were added geometrically, and their parameters constrained to the parent site. The amide group with nitrogen atom N3 was successfully modeled disordered over two positions, with the largest component at 56.4% occupancy.

CCDC 1984323 contains the supplementary crystallographic data of the molecular structures obtained for this paper and can be obtained free of charge via www.ccdc.cam.ac.uk/conts/retrieving.html (or from the Cambridge Crystallographic Data Centre, 12 Union Rd. Cambridge CB2 1EZ, UK; fax: +44-1223-336033; or deposit@ccdc.cam.ac.uk).

2.6. Photophysical characterization

The ligand's ^{1}S and ^{3}T energies were obtained at ~77 K by deconvoluting the fluorescence and phosphorescence spectra of its gadolinium complex into their Franck-Condon progression and are reported as the 0-0 transition [53]. Spectra of the ligand and its complexes were collected at 25.0 ± 0.1 °C using concentrations between 4.0×10^{-5} M and 7.5×10^{-4} M. The formation of $^1O_2$ was monitored by its phosphorescence at 1270 nm.

Emission efficiency measurements. The efficiency of sensitized emission φ^{Ln}, the fluorescence efficiency φ^F, and efficiency of $^1O_2$ generation φ_{1O2} were determined by the dilution method using Equation (1) [54].

$$\varphi_x = \frac{Grad_x}{Grad_{std}} \times \frac{n_x^2}{n_{std}^2} \times \frac{I_{std}}{I_x} \varphi_{std} \quad (1)$$

Grad is the slope of the plot of the emission area as a function of the absorbance, *n* is the refractive index of the solvent, *I* is the intensity of the excitation source at the excitation wavelength used and φ is the quantum yield for sample, *x,* and standard, *std*. All data are the average of at least three independent measurements.

Standards for emission quantum yield measurements were quinine sulfate (φ^F = 55%, 5 × 10$^-$6 M in aqueous 0.5 M H_2SO_4) [55], $Cs_3[Eu(dpa)_3]$ (φ^{Eu} = 24%, 7.5×10^{-5} M in aqueous TRIS/HCl buffer (0.1 M, pH ~7.4)) [56,57], $[Yb(tta)_3(H_2O)_2]$ (φ^{Yb} = 0.12%, 1×10^{-4} M in air-saturated toluene) [58], and 2,2':5',2''-terthiophene (φ_{1O2} = 74%, 1×10^{-4} M in air-saturated acetonitrile) [59] for ligand and Gd^{III} fluorescence, Eu^{III} luminescence, NIR luminescence (Yb^{III}, Nd^{III} and Er^{III}), and $^1O_2$ emission, respectively. The excitation wavelength for both sample and standard were chosen to ensure a linear relationship between the intensity of emitted light and the concentration of the absorbing/emitting species ($A \leq 0.05$).

The intrinsic quantum yield $\varphi_{Eu}^{Eu}$was determined using equation (2).

$$\varphi_{Eu}^{Eu} = \frac{A_{rad}}{A_{tot}} \quad (2)$$

A_{tot} is the total emission rate ($A_{tot} = k_R + k_{NR} = 1/\tau_{exp}$), k_R is the radiative rate constant, k_{NR} is the non-radiative decay constant, τ_{exp} is the observed excited state lifetime, and A_{rad} is the radiative emission rate, determined using equation (3).

$$A_{rad} = A_{MD,0} \times n^3 \left(\frac{I_{tot}}{I_{MD}}\right) \quad (3)$$

$I_{tot}$and I_{MD} are the total integrated emission spectrum and the area of the $^5D_0 \rightarrow {}^7F_1$ transition, respectively, and $A_{MD,0}$ is Einstein coefficient of spontaneous emission ($A_{MD,0}$= 14.65 s^{-1}) [60].

The sensitization efficiency (η_{sens}) was determined using equation (4) [61].

$$\eta_{sens} = \frac{\varphi^{Eu}}{\varphi_{Eu}^{Eu}} \quad (4)$$

3. Results and discussion

3.1. Synthesis and characterization

1Tcbx was synthesized by Suzuki-Miyaura cross-coupling using 4-bromopyridine-2,6-dicarboxamide and 2-thienylboronic acid following modified literature procedures (Fig. S1, supplementary information) [47,62]. After purification, 1Tcbx was recovered in 81% yield as a white powder and was characterized using standard spectroscopic techniques (Fig. S2 – S4). In acetonitrile, 1Tcbx shows an absorption maximum at 305 nm (Fig. S5), with a molar absorptivity (ε) of 2.1×10^4 M^{-1} cm^{-1}. This is similar to other aryl-functionalized thiophene-based compounds [63,64].

1Tcbx crystallized in the P-1 space group as a racemic twin with unit cell parameters a = 7.07 Å, b = 10.15 Å, c = 13.88 Å, V = 954 Å^3, α = 94.28°, β = 97.74°, and γ = 103.33°. Crystallographic details are summarized in Table S1, and selected bond distances and angles are available in Table S2. The compound's structure, shown in Fig. 2, consists of a pyridine ring with biscarboxamide functional groups at the 2- and 6-positions and a thiophene at the 4- position. The torsion angle between the thiophene and pyridine rings (C7–C8–C9–S1) is 9.36(16)°. This angle is similar to what has been reported for 2-thienyl groups in range 3.37°–9.43° [65–68]. We do not observe thiophene-related disorder due to the free rotation between thiophene and bound aryl rings, despite what is often reported in other thiophene-containing molecules [43,44,

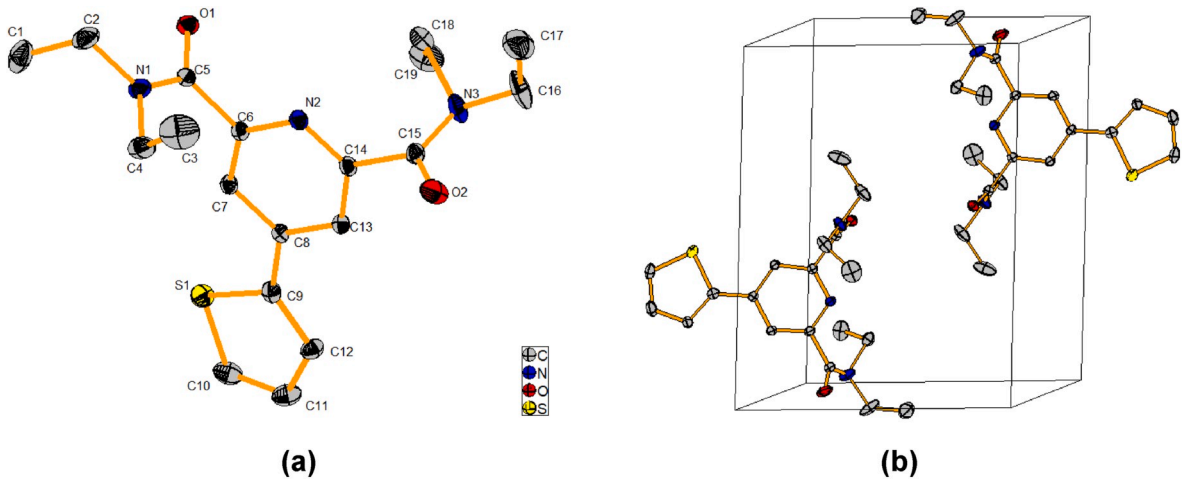

Fig. 2. (a) Thermal ellipsoid plot of 1Tcbx. Ellipsoids are shown at the 50% probability level. (b) Packing structure of 1Tcbx with unit cell edges (black). Hydrogen atoms are omitted for clarity.

69].

3.2. Solution speciation

The stoichiometry of the complexes in solution was determined through absorption titration of the Eu^{III}, Nd^{III}, and Yb^{III} nitrate salts (Figs. S6a, S7a, and S8a) with 1Tcbx. Stability constants are in the ranges 8.6–9.06 (log β_1), 16.76–17.1 (log β_2), and 24.0–24.8 (log β_3) (Table S3). These values are similar to those reported for Ln^{III} complexes with the *N,N,N',N'*-tetraethylpyridine-2,6-dicarboxamide chelator, which are in the range 7.3–8.5 for log β_1, 13.8–16.0 for log β_2, and 21.0–22.9 for log β_3 [70]. Speciation diagrams for complexes of the Ln^{III} ions mentioned above (Figs. S6b, S7b, and S8b) indicate that the 3:1 ligand-to-metal stoichiometry, $[Ln(1Tcbx)_3]^{3+}$, is dominant in solution at the appropriate concentrations. This corresponds to a Ln^{III} ion solely surrounded by three ligands, for a coordination number of 9, as seen for complexes based on the same chelator [70–72].

Therefore, for spectroscopic characterization, Ln^{III} ion complexes were synthesized by reacting 3 equivalents of 1Tcbx with 1 equivalent of the respective $Ln(NO_3)_3$ salt (Ln = Eu^{III}, Nd^{III}, Gd^{III}, Er^{III}, and Yb^{III}) in acetonitrile and used as is. The concentrations were chosen to prevent dissociation which might occur in more dilute solutions [71,72]. After filtration and solvent evaporation, the salts $[Ln(1Tcbx)_3](NO_3)_3$ were obtained as white powders in 92–97% yield and their formation was confirmed by high resolution mass spectrometry (Figs. S9–13).

3.3. Determination of singlet and triplet states of 1Tcbx

Time-resolved emission spectroscopy (Fig. S14a), from which the fluorescence (Fig. S14b) and phosphorescence (Fig. S14c) spectra of $[Gd(1Tcbx)_3]^{3+}$ were obtained, were used to experimentally determine the ligand ^1S and ^3T excited states [53], which are involved in generating $^1O_2$ and sensitizing Ln^{III} luminescence. Deconvolution of the fluorescence and phosphorescence spectra into their Franck-Condon progression allows us to estimate the ^1S and ^3T excited states to be 29,520 cm^{-1} and 23,100 cm^{-1}, respectively (Table 1, Fig. S14). Because the ^3T excited energy state is higher in energy than the $^5D_0$ excited state of Eu^{III} (~17,300 cm^{-1}) and NIR-emitting Ln^{III} ions ($^4F_{3/2}$ of Nd^{III} is ~11,600 cm^{-1}, $^4F_{5/2}$ of Yb^{III} is ~10,300 cm^{-1}, and $^4I_{13/2}$ of Er^{III} is ~6,500 cm^{-1}), we can expect 1Tcbx to sensitize the luminescence of these ions [73,74].

3.4. Absorption and luminescence properties of the complexes

Similar to the absorption behavior of 1Tcbx, the absorption spectra of the metal complexes show a maximum absorption at ~305 nm, with a distinct shoulder around 340 nm. The latter can be attributed to an intraligand CT state that arises upon coordination of the ligand to the metal ions (Fig. S15) [75–77].

When excited at 300 nm, 1Tcbx fluoresces with a maximum at 355 nm (Fig. S5) and a fluorescence quantum yield (φ^F) of 1.0% (Table 1), which compares well with other thiophene-functionalized molecules [64,78–82]. The fluorescence efficiency of $[Gd(1Tcbx)_3]^{3+}$ is the same as 1Tcbx ($\varphi^F = 1\%$) (Table 1, Fig. S156). Although we did not observe an increase in fluorescence intensity upon complexation to Gd^{III} ion, we do observe a 75 nm red shift in the emission maximum. This is consistent with planarization of 1Tcbx upon coordination to Gd^{III}, and increased contribution of the CT state and of phosphorescence due to improved ISC [83] to the emission spectrum. This CT contribution is decreased when the spectrum is obtained at low temperature, as shown in Fig. S17, where the shift in emission maximum is attributed to increased contribution from the ^1S state [84].

Characteristic metal-centered emission is observed for all Ln^{III} complexes when excited at 300 nm, the complex absorption maximum (Fig. 3); Yb^{III}, Nd^{III}, and Er^{III} emit in the NIR region and the Eu^{III} complex

Table 1
Quantum yields of fluorescence (φ^F), quantum yields of sensitized emission (φ^{Ln}), and luminescence lifetimes (τ^{Ln}) of $[Ln(1Tcbx)_3]^{3+}$, singlet (^1S) and triplet (^3T) state energies, intrinsic quantum yield (φ^{Eu}_{Eu}) and sensitization efficiency (η_{sens}) for the Eu^{III} complex.

Compound	λ_{max} (nm)	ε ($M^{-1}cm^{-1}$)	$\varphi^{F/Ln}$ (%)[a]	^1S (cm^{-1})[b]	^3T (cm^{-1})[b]	τ^{Ln}	φ^{Eu}_{Eu} (%)	η_{sens} (%)
1Tcbx	305	2.1×10^4	1 ± 0					
$[Gd(1Tcbx)_3]^{3+}$	306	2.0×10^4	1 ± 1	29,520 ± 100	23,100 ± 230			
$[Eu(1Tcbx)_3]^{3+}$	305	2.3×10^4	25 ± 2			1.11 ± 0.03 ms	47	53
$[Nd(1Tcbx)_3]^{3+}$	304	1.9×10^4	0.19 ± 0.04			3.5 ± 0.3 μs		
$[Yb(1Tcbx)_3]^{3+}$	307	2.0×10^4	0.42 ± 0.05			18.9 ± 0.3 μs		
$[Er(1Tcbx)_3]^{3+}$	305	2.0×10^4	0.01 ± 0.00			–		

[a] Measured at 25.0 ± 0.1 °C.
[b] Measured at 77 K and reported as the 0–0 transition, [complex] = 1×10^{-4} M.

emits in the visible region (Fig. 2, Fig. S19). The emission spectrum of $[Eu(1Tcbx)_3]^{3+}$ displays the characteristic $^5D_0 \rightarrow {}^7F_J$ ($J = 0$–4) transitions. The $^5D_0 \rightarrow {}^7F_2$ transition is a single peak, yet despite the lack of fine structure, the presence of the $^5D_0 \rightarrow {}^7F_0$ transition suggests a pseudo-D_3 symmetry. This is consistent with other reported dipicolinate-based complexes with a 3:1 stoichiometry [10,29]. As indicated by the excitation spectra for the three complexes (Fig. S18), the maximum excitation at 332–335 nm is consistent with sensitization primarily through the CT state [85], contrary to what is generally observed for other emissive Ln^{III} complexes. The quantum yield of sensitized emission (φ^{Eu}) for $[Eu(1Tcbx)_3]^{3+}$ is 25%, the emission decay lifetime (τ^{Eu}) is 1.11 ms (Table 1), and the decay curve could be fit to a single exponential (Fig. S20). From these data, the intrinsic quantum yield ($\varphi\,{}^{Eu}{}_{Eu}$) and the overall sensitization efficiency (η_{sens}) for $[Eu(1Tcbx)_3]^{3+}$ were calculated as 47% and 53%, respectively (Table 1). These values are comparable to similar dipicolinate-based luminescent Eu^{III} complexes [10,56,86]. Although the emission efficiency is lower than the ones determined for the thienyl-derivatized pybox sensitizer [46], we attribute this decrease to the simultaneous generation of $^1O_2$. Nonetheless, φ^{Eu} is among the highest for molecules that show Eu^{III} luminescence and generate $^1O_2$, for which efficiencies in the range 0.3–38% have been reported [27,29,87]. They are comparable to reported values for similar complexes [29,61], and are significantly higher than what we observed for the complexes with the $^1O_2$-generating naphthalimide derivatives [29]. This indicates that 1Tcbx is a moderately good sensitizer and shields the metal ion from vibrational quenching [16].

For $[Nd(1Tcbx)_3]^{3+}$ we observe the typical $^4F_{3/2} \rightarrow {}^4I_J$ ($J = 9/2$–$13/2$) transitions with the most intense transition at 1053 nm, for $[Yb(1Tcbx)_3]^{3+}$ we observe the typical transition $^2F_{5/2} \rightarrow {}^2F_{7/2}$ at 976 nm, and for $[Er(1Tcbx)_3]^{3+}$ we observe the $^4I_{13/2} \rightarrow {}^4I_{15/2}$ transition at 1513 nm (Fig. 3). Quantum yields of NIR luminescence were determined for all three complexes and are $\varphi^{Yb} = 0.42\%$, $\varphi^{Nd} = 0.19\%$, and $\varphi^{Er} = 0.01\%$ (Table 1). These values are comparable to those of other NIR-emitting Yb^{III} and Nd^{III} complexes [30,88–93]. Emission decay lifetimes (τ) were measured for the Yb^{III} and Nd^{III} derivatives and are 18.9 μs and 3.5 μs, respectively, which are comparable as well to lifetimes of other NIR-emitting complexes [94,95]. Both emission decay curves were fit to a single exponential (Figs. S21 and S22), similar to what is observed for the Eu^{III} species, which is consistent with the presence of a single emissive species in solution.

3.5. $^1O_2$ generation

$^1O_2$ emission was observed for all metal complexes, except $[Nd(1Tcbx)_3]^{3+}$, as evidenced by the characteristic phosphorescence band at ~1270 nm (Fig. 4). In the case of the Nd^{III} species, we observe instead the onset of the Nd^{III} transition ($^4F_{3/2} \rightarrow {}^4I_{13/2}$), which overlaps in this region. The intensity of $^1O_2$ phosphorescence is lower when comparing the luminescent compounds of Eu^{III}, Nd^{III}, Yb^{III}, and Er^{III} to the Gd^{III} analog, which does not luminesce, consistent with the competition between Ln^{III} sensitization and $^1O_2$ generation, as both processes involve the triplet excited state ^3T. We have observed a similar decrease with other complexes studied in our group [29,30], as have others [24]. The φ_{1O2} of the Gd^{III} complex is 12 ± 7% and is similar to efficiencies of naturally occurring photosensitizers based on psoralen [96], quinoline [97], phthalocyanine [98], or oligothiophenes [30] in the same solvent. We were unable to quantify φ_{1O2} for the other Ln^{III} complexes and 1Tcbx, due to the low intensity of the $^1O_2$ phosphorescence band at the concentrations needed for the dilution method.

4. Conclusions

A thiophene-functionalized photosensitizer, 1Tcbx, was synthesized, and its Ln^{III} ion complexes were isolated, all of which resulted in compounds with dual functionality. They display metal-centered luminescence and the added capability of generating $^1O_2$, which is a reactive oxygen species known for its toxicity. We demonstrate here the ability to combine $^1O_2$ generators with enhanced luminescence properties, which shows promise for the development of more efficient luminescent complexes with the ability to simultaneously generate $^1O_2$.

The triplet (^3T) state of 1Tcbx is well-matched to sensitize the visible and NIR-emitting Ln^{III} ions (Eu^{III} – visible; Yb^{III}, Nd^{III}, and Er^{III} - NIR). In addition, formation of an intraligand CT state, which is primarily responsible for the sensitization of Ln^{III} emission, was observed. Ln^{III} luminescence efficiencies were as high as 25% for the Eu^{III} analog. This value is one of the highest quantum yields reported for Eu^{III} complexes that also generate $^1O_2$. φ^{Ln} for the NIR emitters are 0.42% for the Yb^{III} complex, 0.15% for the Nd^{III} complex, and 0.01% for the Er^{III} complex. The efficiency of $^1O_2$ generation was determined for $[Gd(1Tcbx)_3]^{3+}$ to be $\varphi_{1O2} = 12\%$. We attribute this high efficiency the heavy atom effect and the inability of the low-lying ^3T state to transfer energy to Gd^{III}. All other complexes generate $^1O_2$, yet the phosphorescence emission at 1270 nm is too weak to allow us to determine the efficiency of this process, as the ^3T state of 1Tcbx is involved in the concurrent sensitization of the metal-centered emission. The findings presented here show that functionalization of an antenna with a substituent known to generate $^1O_2$, such as thiophene, offers a new approach to conserving

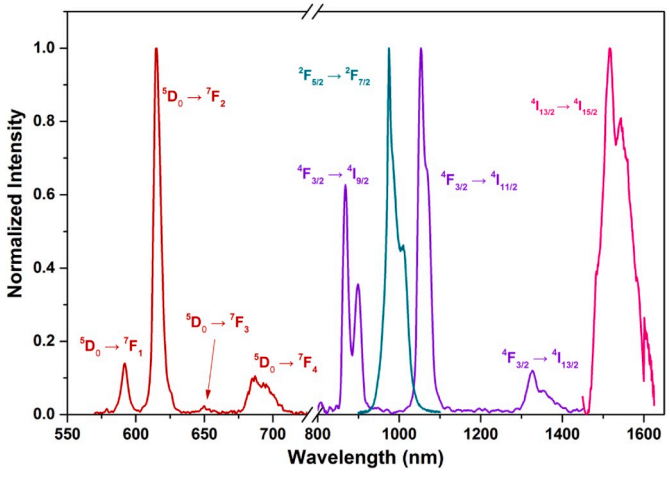

Fig. 3. Emission spectra of the $[Ln(1Tcbx)_3]^{3+}$ complexes (Ln = Eu^{III} (red), Nd^{III} (purple), Yb^{III}(teal) and Er^{III} (pink)) in acetonitrile at 25.0 ± 0.1 °C (λ_{exc} = 300 nm).

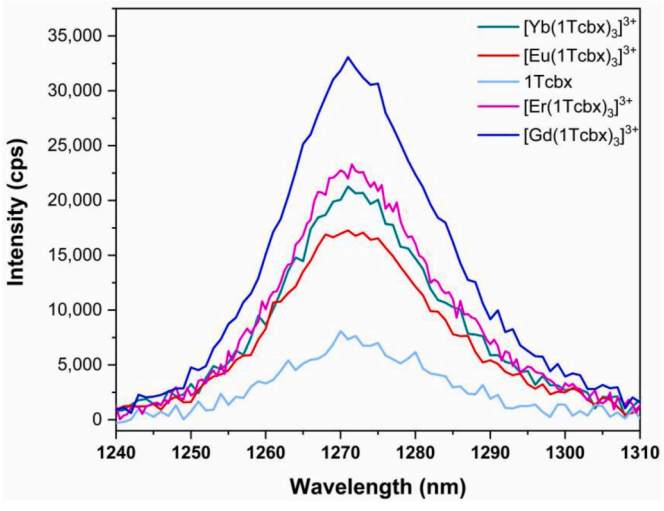

Fig. 4. $^1O_2$ emission spectra of 1Tcbx (light blue) and metal complexes (Ln^{III} = Eu^{III} (red), Gd^{III} (dark blue), Er^{III} (pink), and Yb^{III}(teal)) in acetonitrile at 25.0 ± 0.01 °C. [compound] = 5×10^{-4} M, (λ_{exc} = 335 nm).

luminescence efficiency while also adding $^1O_2$ generating capability.

Author statement

The first author (KRJ) performed most of the experiments and interpreted, with the support of the corresponding author (AdBD) the data collected. The second author (MAGN) synthesized the ligand for the first time and did limited ligand characterization. The corresponding author guided the development of the research project, and supervised the experimental work and writing of the manuscript.

Declaration of competing interest

There are no conflicts of interest to declare.

Acknowledgments

Financial support of this work through the National Science Foundation is gratefully acknowledged (Grant CHE 1800392).

Appendix A. Supplementary data

Supplementary data to this article can be found online at https://doi.org/10.1016/j.jlumin.2020.117309.

References

[1] K. Iman, M. Shahid, Life sensors: current advances in oxygen sensing by lanthanide complexes, New J. Chem. 43 (2019) 1094–1116.
[2] U. Cho, D.P. Riordan, P. Ciepla, K.S. Kocherlakota, J.K. Chen, P.B. Harbury, Ultrasensitive optical imaging with lanthanide lumiphores, Nat. Chem. Biol. 14 (2017) 15–21.
[3] J. Lehr, M. Tropiano, P.D. Beer, S. Faulkner, J.J. Davis, Ratiometric oxygen sensing using lanthanide luminescent emitting interfaces, Chem. Commun. 51 (2015) 15944–15947.
[4] J.-C.G. Bünzli, C. Piguet, Taking advantage of luminescent lanthanide ions, Chem. Soc. Rev. 34 (2005) 1048–1077.
[5] J.-C.G. Bunzli, Luminescence bioimaging with lanthanide complexes, Luminescence of Lanthanide Ions in Coordination Compounds and Nanomaterials (2014) 125–196.
[6] J.-C.G. Bünzli, A.-S. Chauvin, C.D.B. Vandevyver, S. Bo, S. Comby, Lanthanide bimetallic helicates for in vitro imaging and sensing, Ann. N. Y. Acad. Sci. 1130 (2008) 97–105.
[7] J.-C.G. Bünzli, C. Piguet, Taking advantage of luminescent lanthanide ions, Chem. Soc. Rev. 34 (2005) 1048–1077.
[8] Y. Fang, W. Shi, Y. Hu, X. Li, H. Ma, A dual-function fluorescent probe for monitoring the degrees of hypoxia in living cells via the imaging of nitroreductase and adenosine triphosphate, Chem. Commun. 54 (2018) 5454–5457.
[9] Y. Ning, J. Tang, Y.-W. Liu, J. Jing, Y. Sun, J.-L. Zhang, Highly luminescent, biocompatible ytterbium(iii) complexes as near-infrared fluorophores for living cell imaging, Chem. Sci. 9 (2018) 3742–3753.
[10] J.H.S.K. Monteiro, D. Machado, L.M. de Hollanda, M. Lancellotti, F.A. Sigoli, A. de Bettencourt-Dias, Selective cytotoxicity and luminescence imaging of cancer cells with a dipicolinato-based EuIII complex, Chem. Commun. 53 (2017) 11818–11821.
[11] I. Martinić, S.V. Eliseeva, T.N. Nguyen, V.L. Pecoraro, S. Petoud, Near-infrared optical imaging of necrotic cells by photostable lanthanide-based metallacrowns, J. Am. Chem. Soc. 139 (2017) 8388–8391.
[12] X. Wu, X. Sun, Z. Guo, J. Tang, Y. Shen, T.D. James, H. Tian, W. Zhu, In vivo and in situ tracking cancer chemotherapy by highly photostable NIR fluorescent theranostic prodrug, J. Am. Chem. Soc. 136 (2014) 3579–3588.
[13] J.-C.G. Bünzli, Lanthanide luminescence for biomedical analyses and imaging, Chem. Rev. 110 (2010) 2729–2755.
[14] J.-C.G. Bünzli, G.R. Choppin, Lanthanide Probes in Life, Chemical and Earth Sciences - Theory and Practice, Elsevier, Amsterdam, 1989.
[15] V.S. Sastri, J.C. Bünzli, J.R. Perumareddi, V.R. Rao, G.V.S. Rayudu, Modern Aspects of Rare Earths and Their Complexes, Elsevier, 2003, p. 956.
[16] A. de Bettencourt-Dias, in: A. de Bettencourt-Dias (Ed.), Introduction to Lanthanide Ion Luminescence in *Luminescence Of Lanthanide Ions In Coordination Compounds And Nanomaterials*, John Wiley & Sons, Ltd., Chichester, United Kingdom, 2014, pp. 1–48.
[17] G.A. Hebbink, S.I. Klink, L. Grave, P.G.B. Oude Alink, F.C.J.M. Van Veggel, Singlet energy transfer as the main pathway in the sensitization of near-infrared Nd3+ luminescence by dansyl and lissamine dyes, ChemPhysChem 3 (2002) 1014–1018.
[18] J.B. Lamture, Z.H. Zhou, A.S. Kumar, T.G. Wensel, Luminescence properties of terbium(III) complexes with 4-substituted dipicolinic acid analogs, Inorg. Chem. 34 (1995) 864–869.
[19] A. D'Aleo, F. Pointillart, L. Ouahab, C. Andraud, O. Maury, Charge transfer excited states sensitization of lanthanide emitting from the visible to the near-infra-red, Coord. Chem. Rev. 256 (2012) 1604–1620.
[20] A.R. Lippert, T. Gschneidtner, C.J. Chang, Lanthanide-based luminescent probes for selective time-gated detection of hydrogen peroxide in water and in living cells, Chem. Commun. 46 (2010) 7510–7512.
[21] S. Sato, A. Ishii, C. Yamada, J. Kim, C. Ho Song, A. Fujiwara, M. Takata, M. Hasegawa, Luminescence of fusion materials of polymeric chain-structured lanthanide complexes, Polym. J. 47 (2015) 195–200.
[22] A. Watkis, R. Hueting, T.J. Sørensen, M. Tropiano, S. Faulkner, Controlling energy transfer in ytterbium complexes: oxygen dependent lanthanide luminescence and singlet oxygen formation, Chem. Commun. 51 (2015) 15633–15636.
[23] J.-X. Zhang, W.-L. Chan, C. Xie, Y. Zhou, H.-F. Chau, P. Maity, G.T. Harrison, A. Amassian, O.F. Mohammed, P.A. Tanner, W.-K. Wong, K.-L. Wong, Impressive near-infrared brightness and singlet oxygen generation from strategic lanthanide–porphyrin double-decker complexes in aqueous solution, Light Sci. Appl. 8 (2019) 46.
[24] M. Galland, F. Riobé, J. Ouyang, N. Saleh, F. Pointillart, V. Dorcet, B. Le Guennic, O. Cador, J. Crassous, C. Andraud, C. Monnereau, O. Maury, Helicenic complexes of lanthanides: influence of the f-element on the intersystem crossing efficiency and competition between luminescence and oxygen sensitization, Eur. J. Inorg. Chem. 2019 (2019) 118–125.
[25] K. Singh, S. Banerjee, A.K. Patra, Photocytotoxic luminescent lanthanide complexes of DTPA–bisamide using quinoline as photosensitizer, RSC Adv. 5 (2015) 107503–107513.
[26] M. Galland, T. LeBahers, A. Banyasz, N. Lascoux, A. Duperray, A. Grichine, R. Tripier, Y. Guyot, M. Maynadier, C. Nguyen, M. Gary-Bobo, C. Andraud, C. Monnereau, O. Maury, A "multi-heavy-atom" approach toward biphotonic photosensitizers with improved singlet-oxygen generation properties, Chem. Eur J. (2019), 0.
[27] S. Dasari, A.K. Patra, Luminescent europium and terbium complexes of dipyridoquinoxaline and dipyridophenazine ligands as photosensitizing antennae: structures and biological perspectives, Dalton Trans. 44 (2015) 19844–19855.
[28] D.J. Toffoli, L. Gomes, N.D. Vieira Jr., L.C. Courrol, Photodynamic potentiality of hypocrellin B and its lanthanide complexes, J. Opt. A Pure Appl. Op. 10 (2008) 104026.
[29] K.R. Johnson, A. de Bettencourt-Dias, 1O2 generating luminescent lanthanide complexes with 1,8-naphthalimide-based sensitizers, Inorg. Chem. 58 (2019) 13471–13480.
[30] K.R. Johnson, S.B. Vittardi, M.A. Gracia-Nava, J.J. Rack, A. de Bettencourt-Dias, Wavelength-dependent singlet oxygen generation in luminescent lanthanide complexes with a pyridine-bis(carboxamide)-terthiophene sensitizer, Chem. Eur J. (2020) (Accepted).
[31] K.R. Johnson, V.C. Lombardi, A. de Bettencourt-Dias, Photocytotoxicity of Oligothienyl-functionalized Chelates that Sensitize Ln^{III} Luminescence and Generate $^1O_2$, Chem. Eur. J. (2020), https://doi.org/10.1002/chem.202001568.
[32] J. Kagan, K. Tadema-Wielandt, G. Chan, S.N. Dhawan, J. Jaworsky, I. Prakash, S. K. Arora, Oxygen requirement for near-UV mediated cytotoxicity of phenylheptatriyne to Escherichia coli, Photochem. Photobiol. 39 (1984) 465–467.
[33] J.T. Arnason, B.J.R. Philogéne, C. Berg, A. MacEachern, J. Kaminski, L.C. Leitch, P. Morand, J. Lam, Phototoxicity of naturally occurring and synthetic thiophene and acetylene analogues to mosquito larvae, Phytochemistry 25 (1986) 1609–1611.
[34] J.T. Arnason, B.J.R. Philogène, P. Morand, K. Imrie, S. Iyengar, F. Duval, C. Soucy-Breau, J.C. Scaiano, N.H. Werstiuk, B. Hasspieler, A.E.R. Downe, Naturally occurring and synthetic thiophenes as photoactivated insecticides, in: Insecticides of Plant Origin, vol. 387, American Chemical Society, 1989, pp. 164–172.
[35] R.J. Marles, R.L. Compadre, C.M. Compadre, C. Soucy-Breau, R.W. Redmond, F. Duval, B. Mehta, P. Morand, J.C. Scaiano, J.T. Arnason, Thiophenes as mosquito larvicides: structure-toxicity relationship analysis, Pestic. Biochem. Physiol. 41 (1991) 89–100.
[36] J. Kagan, J.-P. Beny, G. Chan, S.N. Dhawan, J.A. Jaworski, E.D. Kagan, P. D. Kassner, M. Murphy, J.A. Rogers, The phototoxicity of some 1,3-butadienes and related thiophenes against larvae of the mosquito Aedes aegypti and of the fruit fly Drosophila melanogaster, Int. J. Trop. Insect Sci. 4 (1983) 377–381.
[37] T. Arnason, G.F.Q. Chan, C.K. Wat, K. Downum, G.H.N. Towers, Oxygen requirement for near-UV mediated cytotoxicity of α-terthienyl to Escherichia coli and Saccharomyces cerevisiae *photochem*, Photobiol 33 (1981) 821–824.
[38] C. Romagnoli, D. Mares, M.P. Fasulo, A. Bruni, Antifungal effects of α-terthienyl from Tagetes patula on five dermatophytes, Phytother Res. 8 (1994) 332–336.
[39] J.B. Hudson, L. Harris, A. Teeple, G.H.N. Towers, The anti-HIV activity of the phytochemical α-terthienyl, Antivir. Res. 20 (1993) 33–43.
[40] J.B. Hudson, E.A. Graham, N. Miki, G.H.N. Towers, L.L. Hudson, R. Rossi, A. Carpita, D. Neri, Photoactive antiviral and cytotoxic activities of synthetic thiophenes and their acetylenic derivatives, Chemosphere 19 (1989) 1329–1343.
[41] J.B. Hudson, E.A. Graham, N. Micki, L. Hudson, G.H.N. Towers, Antiviral activity of the photoactive thiophene α-terthienyl, Photochem. Photobiol. 44 (1986) 477–482.
[42] X. Song, M.G. Fanelli, J.M. Cook, F. Bai, C.A. Parish, Mechanisms for the reaction of thiophene and methylthiophene with singlet and triplet molecular oxygen, J. Phys. Chem. 116 (2012) 4934–4946.
[43] A. de Bettencourt Dias, S. Viswanathan, Luminescent Ln3+ nitrobenzoato complexes: first examples of sensitization of green and red emission, Chem. Commun. (2004) 1024–1025.

[44] A. de Bettencourt-Dias, S. Viswanathan, K. Ruddy, Intermolecular forces and functional group effects in the packing structure of thiophene derivatives, Cryst. Growth Des. 5 (2005) 1477–1483.
[45] S. Viswanathan, A. de Bettencourt-Dias, Eu(III) and Tb(III) luminescence sensitized by thiophenyl-derivatized nitrobenzoato antennas, Inorg. Chem. 45 (2006) 10138–10146.
[46] A. de Bettencourt-Dias, S. Viswanathan, A. Rollett, Thiophene-derivatized pybox and its highly luminescent lanthanide ion complexes, J. Am. Chem. Soc. 129 (2007) 15436–15437.
[47] G. Muller, B. Schmidt, J. Jiricek, G. Hopfgartner, J.P. Riehl, J.-C.G. Bunzli, C. Piguet, Lanthanide triple helical complexes with a chiral ligand derived from 2,6-pyridinedicarboxylic acid, Dalton Trans. (2001) 2655–2662.
[48] S. Rihn, P. Retailleau, A. De Nicola, G. Ulrich, R. Ziessel, Synthetic routes to fluorescent dyes exhibiting large Stokes shifts, J. Org. Chem. 77 (2012) 8851–8863.
[49] P. Gans, A. Sabatini, A. Vacca, Investigation of equilibria in solution. Determination of equilibrium constants with the HYPERQUAD suite of programs, Talanta 43 (1996) 1739–1753.
[50] L. Alderighi, P. Gans, A. Ienco, D. Peters, A. Sabatini, A. Vacca, Hyperquad simulation and speciation (HySS): a utility program for the investigation of equilibria involving soluble and partially soluble species, Coord. Chem. Rev. 184 (1999) 311–318.
[51] SADABS: v. 2.01, An Empirical Absorption Correction Program, Bruker AXS Inc., Madison, WI., 2001.
[52] SHELXTL: v, 6.10 Structure Determination Software Suite, Bruker AXS Inc., Madison, WI., 2001.
[53] G.A. Crosby, R.E. Whan, R.M. Alire, Intramolecular energy transfer in rare earth chelates. Role of the triplet state, J. Chem. Phys. 34 (1961) 743–748.
[54] P.H.H. Hänninen, Lanthanide Luminescence Photophysical, Analytical and Biological Aspects, 1 ed., Springer-Verlag Berlin Heidelberg, 2011.
[55] W.H. Melhuish, Quantum efficiencies of fluorescence of organic substances: effect of solvent and concentration of the fluorescent solute, J. Phys. Chem. 65 (1961) 229–235.
[56] A.S. Chauvin, F. Gumy, D. Imbert, J.C.G. Bünzli, Europium and terbium tris (dipicolinates) as secondary standards for quantum yield determination, Spectrosc. Lett. 37 (2004) 517–532.
[57] Erratum. *Spectrosc. Lett.* 40 (2007), 193-193.
[58] M.P. Tsvirko, S.B. Meshkova, V.Y. Venchikov, Z.M. Topilova, D.V. Bol'shoi, Determination of contributions of various molecular groups to nonradiative deactivation of electronic excitation energy in beta-diketonate complexes of ytterbium(III), Optic Spectrosc. 90 (2001) 669–673.
[59] R.S. Becker, J. Seixas de Melo, A.L. Maçanita, F. Elisei, Comprehensive evaluation of the absorption, photophysical, energy transfer, structural, and theoretical properties of α-oligothiophenes with one to seven rings, J. Phys. Chem. 100 (1996) 18683–18695.
[60] Sá de, G F, O.L. Malta, C. de Mello Donegá, A.M. Simas, R.L. Longo, P.A. Santa-Cruz, E.F. da Silva, Spectroscopic properties and design of highly luminescent lanthanide coordination complexes, Coord. Chem. Rev. 196 (2000) 165–195.
[61] A. Aebischer, F. Gumy, J.-C.G. Bünzli, Intrinsic quantum yields and radiative lifetimes of lanthanide tris(dipicolinates), Phys. Chem. Chem. Phys. 11 (2009) 1346–1353.
[62] D.-S. Kim, K.H. Ahn, Fluorescence "turn-on" sensing of carboxylate anions with oligothiophene-based o-(carboxamido)trifluoroacetophenones, J. Org. Chem. 73 (2008) 6831–6834.
[63] A. Tabet, A. Schröder, H. Hartmann, D. Rohde, L. Dunsch, Preparation and characterization of α,α'-bisdiarylamino-capped oligothiophenes, Org. Lett. 5 (2003) 1817–1820.
[64] M. Manuela, M. Raposo, C. Herbivo, V. Hugues, G. Clermont, M.C.R. Castro, A. Comel, M. Blanchard-Desce, Synthesis, fluorescence, and two-photon absorption properties of push–pull 5-Arylthieno[3,2-b]thiophene derivatives, Eur. J. Org Chem. 2016 (2016) 5263–5273.
[65] S. Encinas, L. Flamigni, F. Barigelletti, E.C. Constable, C.E. Housecroft, E. R. Schofield, E. Figgemeier, D. Fenske, M. Neuburger, J.G. Vos, M. Zehnder, Electronic energy transfer and collection in luminescent molecular rods containing ruthenium(II) and osmium(II) 2,2′:6′,2″-terpyridine complexes linked by thiophene-2,5-diyl spacers, Chem. Eur J. 8 (2002) 137–150.
[66] A. Maroń, S. Kula, A. Szlapa-Kula, A. Świtlicka, B. Machura, S. Krompiec, J. G. Małecki, R. Kruszyński, A. Chrobok, E. Schab-Balcerzak, S. Kotowicz, M. Siwy, K. Smolarek, S. Maćkowski, H. Janeczek, M. Libera, 2,2′:6′,2″-Terpyridine analogues: structural, electrochemical, and photophysical properties of 2,6-Di (thiazol-2-yl)pyridine derivatives, Eur. J. Org Chem. 2017 (2017) 2730–2745.
[67] D.C. Young, H. Yang, S.G. Telfer, P.E. Kruger, An isoreticular series of zinc(II) metal–organic frameworks derived from terpyridylcarboxylate ligands, Inorg. Chem. 56 (2017) 12224–12231.
[68] A. de Bettencourt-Dias, A. Poloukhtine, Phenylthiophene−Dipicolinic acid-based emitters with strong solution blue and solid state green emission, J. Phys. Chem. B 110 (2006) 25638–25645.
[69] S.V. Rocha, N.S. Finney, Systematic evaluation of 2,6-linked pyridine–thiophene oligomers, J. Org. Chem. 78 (2013) 11255–11261.
[70] F. Renaud, C. Piguet, G. Bernardinelli, J.-C.G. Bünzli, G. Hopfgartner, In search for mononuclear helical lanthanide building blocks with predetermined properties: triple-stranded helical complexes with N,N,N',N'-tetraethylpyridine-2,6-dicarboxamide, Chem. Eur J. 3 (1997) 1646–1659.
[71] F. Renaud, C. Piguet, G. Bernardinelli, J.-C.G. Bünzli, G. Hopfgartner, In search for mononuclear helical lanthanide building blocks with predetermined properties: triple-stranded helical complexes with N,N,N',N'-tetraethylpyridine-2,6-dicarboxamide, Chem. Eur J. 3 (1997) 1646–1659.
[72] A. Picot, F. Malvolti, B. Le Guennic, P.L. Baldeck, J.A.G. Williams, C. Andraud, O. Maury, Two-photon antenna effect induced in octupolar europium complexes, Inorg. Chem. 46 (2007) 2659–2665.
[73] W.T. Carnall, P.R. Fields, B.G. Wybourne, Electronic energy levels in the trivalent lanthanide aquo ions. I. Pr3+, Nd3+, Pm3+, Sm3+, Dy3+, Ho3+, Er3+, and Tm3+, J. Chem. Phys. 49 (1968) 4424.
[74] W.T. Carnall, P.R. Fields, K. Rajnak, Electronic energy levels of the trivalent lanthanide aquo ions. IV. Eu3+, J. Chem. Phys. 49 (1968) 4450–4455.
[75] F. Pointillart, A. Bourdolle, T. Cauchy, O. Maury, Y. Le Gal, S. Golhen, O. Cador, L. Ouahab, In solution sensitization of Er(III) luminescence by the 4-Tetrathiafulvalene-2,6-pyridinedicarboxylic acid dimethyl antenna ligand, Inorg. Chem. 51 (2012) 978–984.
[76] J.H.S.K. Monteiro, N.R. Fetto, M.J. Tucker, A. de Bettencourt Dias, Complexes with high two-photon absorption cross-section enable viscosity-sensing in the visible and near IR with one- and two-photon excitation, Inorg. Chem. 59 (2020) 3193–3199.
[77] J.H.S.K. Monteiro, F.A. Sigoli, A. de Bettencourt-Dias, A Water-soluble Tb^{III} complex as temperature-sensitive luminescent probe, Can. J. Chem. 96 (2018) 859–864.
[78] H. Mo, K.R. Radke, K. Ogawa, C.L. Heth, B.T. Erpelding, S.C. Rasmussen, Solution and solid-state properties of highly fluorescent dithieno[3,2-b:2[prime or minute],3[prime or minute]-d]pyrrole-based oligothiophenes, Phys. Chem. Chem. Phys. 12 (2010) 14585–14595.
[79] L. Ren, F. Liu, X. Shen, C. Zhang, Y. Yi, X. Zhu, Developing quinoidal fluorophores with unusually strong red/near-infrared emission, J. Am. Chem. Soc. 137 (2015) 11294–11302.
[80] J. Pina, J.S. Seixas de Melo, R.M.F. Batista, S.P.G. Costa, M.M.M. Raposo, Synthesis and characterization of the ground and excited states of tripodal-like oligothienyl-imidazoles, J. Phys. Chem. B 114 (2010) 4964–4972.
[81] J. Seixas de Melo, L.M. Silva, M. Kuroda, Photophysical and theoretical studies of naphthalene-substituted oligothiophenes, J. Chem. Phys. 115 (2001) 5625–5636.
[82] J. Seixas de Melo, H.D. Burrows, M. Svensson, M.R. Andersson, A.P. Monkman, Photophysics of thiophene based polymers in solution: the role of nonradiative decay processes, J. Chem. Phys. 118 (2003) 1550–1556.
[83] C.-C. Ko, V.W.-W. Yam, Coordination compounds with photochromic ligands: ready tunability and visible light-sensitized photochromism, Acc. Chem. Res. 51 (2018) 149–159.
[84] A. Picot, F. Malvolti, B. Le Guennic, P.L. Baldeck, J.A. Gareth Williams, C. Andraud, O. Maury, Two-photon antenna effect induced in octupolar europium complexes, Inorg. Chem. 46 (2007) 2659–2665.
[85] A. Picot, A. D'Aléo, P.L. Baldeck, A. Grichine, A. Duperray, C. Andraud, O. Maury, Long-lived two-photon excited luminescence of water-soluble europium complex: applications in biological imaging using two-photon scanning microscopy, J. Am. Chem. Soc. 130 (2008) 1532–1533.
[86] A.-S. Chauvin, F. Gumy, D. Imbert, J.-C.G. Bunzli, Erratum. *Spectrosc. Lett.* 40 (2007), 193-193.
[87] G. Bobba, Y. Bretonnière, J.-C. Frias, D. Parker, Enantiopure lanthanide complexes incorporating a tetraazatriphenylene sensitiser and three naphthyl groups: exciton coupling, intramolecular energy transfer, efficient singlet oxygen formation and perturbation by DNA binding, Org. Biomol. Chem. 1 (2003) 1870–1872.
[88] J. Zhang, D. Badger Paul, J. Geib Steven, S. Petoud, Sensitization of near-infrared-emitting lanthanide cations in solution by tropolonate ligands, Angew. Chem. 44 (2005) 2508–2512.
[89] D. Kovacs, X. Lu, L.S. Mészáros, M. Ott, J. Andres, K.E. Borbas, Photophysics of coumarin and carbostyril-sensitized luminescent lanthanide complexes: implications for complex design in multiplex detection, J. Am. Chem. Soc. 139 (2017) 5756–5767.
[90] C.Y. Chow, S.V. Eliseeva, E.R. Trivedi, T.N. Nguyen, J.W. Kampf, S. Petoud, V. L. Pecoraro, Ga3+/Ln3+ metallacrowns: a promising family of highly luminescent lanthanide complexes that covers visible and near-infrared domains, J. Am. Chem. Soc. 138 (2016) 5100–5109.
[91] Z. Ahmed, K. Iftikhar, Sensitization of visible and NIR emitting lanthanide(III) ions in noncentrosymmetric complexes of hexafluoroacetylacetone and unsubstituted monodentate pyrazole, J. Phys. Chem. 117 (2013) 11183–11201.
[92] N.M. Shavaleev, S.J.A. Pope, Z.R. Bell, S. Faulkner, M.D. Ward, Visible-light sensitisation of near-infrared luminescence from Yb(iii), Nd(iii) and Er(iii) complexes of 3,6-bis(2-pyridyl)tetrazine, Dalton Trans. (2003) 808–814.
[93] N.S. Baek, Y.H. Kim, Y.K. Eom, J.H. Oh, H.K. Kim, A. Aebischer, F. Gumy, A.-S. Chauvin, J.-C.G. Bunzli, Sensitized near-IR luminescence of lanthanide complexes based on push-pull diketone derivatives, Dalton Trans. 39 (2010) 1532–1538.
[94] Y. Hasegawa, T. Matsui, Y. Kitagawa, T. Nakanishi, T. Seki, H. Ito, Y. Nakasaka, T. Masuda, K. Fushimi, Near-IR luminescent YbIII coordination polymers composed of pyrene derivatives for thermostable oxygen sensors, Chem. Eur J. 25 (2019) 12308–12315.
[95] Y. Hasegawa, T. Ohkubo, K. Sogabe, Y. Kawamura, Y. Wada, N. Nakashima, S. Yanagida, Luminescence of novel neodymium sulfonylaminate complexes in organic media, Angew. Chem. 39 (2000) 357–360.

[96] A. Losi, R. Bedotti, C. Viappiani, Time-resolved photoacoustics determination of intersystem crossing and singlet oxygen photosensitization quantum yields for 4,5',8-trimethylpsoralen, J. Phys. Chem. 99 (1995) 16162–16167.
[97] K. Gollnick, S. Held, D.O. Mártire, S.E. Braslavsky, Hydroxyanthraquinones as sensitizers of singlet oxygen reactions: quantum yields of triplet formation and singlet oxygen generation in acetonitrile, J. Photochem. Photobiol., A 69 (1992) 155–165.
[98] S. Foley, G. Jones, R. Liuzzi, J. McGarvey, D, H. Perry, M, T. George Truscott, The synthesis and photophysical properties of polyether substituted phthalocyanines of potential use in photodynamic therapy, Perkin Trans (1997) 1725–1730.